공학석사 학위논문

# A study on the sound reduction of slits with an acoustic sealant

## 방음용 실란트를 이용한 틈새 소음 저감에 대한 연구

2023년 2월

서울대학교 대학원
기계공학부

하 헌 주

# 방음용 실란트를 이용한 틈새 소음 저감에 대한 연구

**A study on the sound reduction of slits with an acoustic sealant**

지도교수 강 연 준

이 논문을 공학석사 학위논문으로 제출함

2022 년 10 월

서울대학교 대학원
기계공학부
하 헌 주

하헌주의 공학석사 학위논문을 인준함

2022 년 12 월

위 원 장 : 도 형 록

부위원장 : 강 연 준

위 원 : 김 도 년

# ABSTRACT

# A study on the sound reduction of slits with an acoustic sealant

Heon Ju Ha
School of Mechanical Engineering
The Graduate School
Seoul National University

Lightweight walls can be easily installed for the purpose of separating spaces and blocking noise indoors. These walls are non-bearing walls, —since these structures are installed in addition to the existing structures. Joint sections between old and new structures form apertures. These apertures, which include floors, ceilings, windows, and doors, —hinder soundproofing and fireproofing performance. These defects are reduced by filling these apertures with sealants. Among the sealants, an acoustic sealant serves to block generated noise in this manner.

This study conducts a theoretical analysis of acoustic transmission according to the presence or absence of an acoustic sealant for apertures in lightweight walls. Also, it verifies the validity of the theory by measuring transmission loss using the sound intensity technique. The theory uses a Mechel prediction model rather than

Gomperts and Kiliman, which have been primarily employed in earlier studies.

The proposed model has very good agreement with the measurement value, with a difference of less than $2dB$. The theory is restricted when the transmission coefficients of partition and sealant are not significantly different. However, the slit with an acoustic sealant represents an equivalent sound reduction effect, —which is a wall without a slit.

**Keywords :** Indoor noise, Flanking transmission, Slit, Acoustic seal
**Student Number :** 2021−27018

# TABLE OF CONTENTS

# LIST OF TABLES

# LIST OF FIGURES

# CHAPTER 1

# INTRODUCTION

The desire to improve noise problems in residential environments has increased to meet the needs of improving quality of life and personal privacy. The goals have led to improvements in construction materials and methods, such as absorbent materials with excellent sound insulation performance. One of the methods is installing lightweight walls, which are characterized by easy construction and high transmission loss.

The sound transmission paths of the walls are classified as direct and indirect. The direct way is through the transmission of the walls toward the receiver. The other way is through flanking transmissions, which are located in ceilings, floors, doors, windows, —and other apertures. The flanking noise affects the sound reduction capacity of walls. Acoustic sealants and absorbent materials in apertures are used to reduce the noise problems.

Aperture terms are used comprehensively, but they can be classified according to their size, —shape. It is defined as a "leak" with an aperture smaller than the wavelength of sound. The opposite case is defined as "opening". Both are commonly referred to as "aperture" [1]. Also, the rectangular shape of an aperture is called a "slit".

Numerous methods have been used to study the sound transmission through an aperture so far. The theoretical studies included Gomperts [2], Gomperts and Kihlman [3], Wilson and

Soroka [4], Sauter and Soroka [5], Mechel [6], Chen [7], Yang et al [8], and numerical studies included Park and Eom [9], Sgard et al [1], Poblet-Puig, —and Rodriguez-Ferran [10]. The experimental studies included Oldham and Jhao [11], Hongisto [12], Uris et al. [13], and Kim [14].

Few analytical and experimental research have been counducted on apertures with particular sealing materials. In addition, most of the previous studies used a prediction model by Gomperts and Kihlman [3], whereas this study utilizes a prediction model by Mechel [6].

The present paper proposes a prediction model for transmission loss for gypsum boards with slits, —and confirms the effect obtained by filling the slits with acoustic sealant. This prediction model is verified by comparing it with the experiment.

This thesis is organized as follows: In Section 2, the prediction model that calculates the sound transmission through a slit is presented, including Fahy's model [15] and Mechel's model [6]. In Section 3, the experimental arrangement and results are described. In Section 4, the prediction model is compared with the experimental result. Finally, conclusions and future work are drawn in Section 5 to conclude the thesis.

# CHAPTER 2

# THEORY

## 2.1. Theoretical model for sound transmission

Consider a slit located at the center of the wall, which is infinitely baffled and of finite thickness for theoretical ease. Assume that surface motion is like a piston. An oblique plane wave penetrates the partition and slit. Figure 2.1 represents the transmission paths of the wall. The transmission coefficient of total sound is calculated as the sum of the products of the transmission coefficient and the area ratio, respectively.

$$\tau_{total} = \tau_{slit}\left(\frac{S_{slit}}{S_{total}}\right) + \tau_{partition}\left(\frac{S_{partition}}{S_{total}}\right). \tag{2.1}$$

The sound transmission coefficient through a slit, $\tau_{slit}$, is calculated by a modified model, which is Mechel's model [6] for a slit. Also, the sound transmission coefficient through a partition, $\tau_{partition}$, is predicted by Fahy's model [15].

$$\tau_{partition} = \frac{(2\rho_0 c/\omega m)^2 \sec^2\theta_i}{[(2\rho_0 c \sec\theta_i/\omega m) + (k_0 \sin\theta_i/k_b)^4\eta]^2 + [1-(k_0\sin\theta_i/k_b)^4]^2} \tag{2.2}$$

where $k_b = (\omega^2 m/D)^{1/4}$ is the flexural wavenumber in a partition, $D$ is the bending rigidity, and $\eta$ is damping factor.

The total transmission coefficient of the wall can be obtained by substituting Eq.(2.1) with the respective transmission coefficients and area ratios.

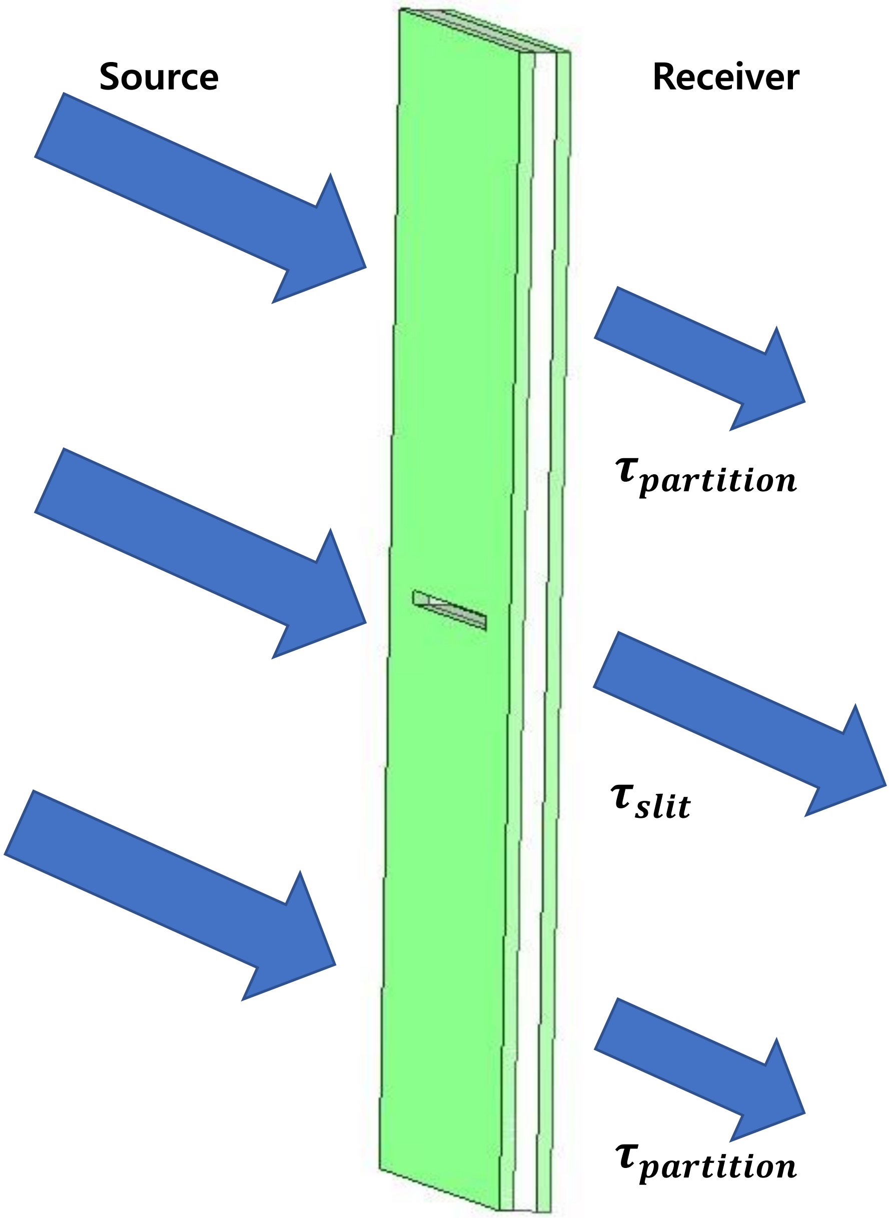


Figure 2.1 —The transmission paths of the wall

## 2.2. Theoretical model for a slit

A slit that consists of a single medium is transmitted by an obliquely incident plane wave in Figure 2.2. The incident wave, $P_{i,1}$, may reach the slit at an angle $\phi_1$ in orthogonal coordinates to the x−axis, which is parallel to the slit surface. The angle to the z−axis, which is normal to the slit surface, —is $\theta_1$.

The equation representing the sound pressure field for each compartment excluding the time harmonic factor $e^{j\omega t}$ is as follows. The pressure field in 1 is determined by the superposition of the blocked pressure and radiated pressure, which are caused by the virtual baffled piston,

$$P_1 = P_{i,1} + P_{r,1} + P_{rad,1} = P_{block} + P_{rad,1}, \tag{2.3}$$

$$P_{i,1}(x,y,z) = \hat{P}_1 e^{-jk_0(x\sin\theta_1\cos\phi_1 + y\sin\theta_1\cos\phi_1 + z\cos\theta_1)}, \text{ and} \tag{2.4}$$

$$P_{r,1}(x,y,z) = \hat{P}_1 e^{-jk_0(x\sin\theta_1\cos\phi_1 + y\sin\theta_1\cos\phi_1 - z\cos\theta_1)}, \tag{2.5}$$

where $P_{i,1}$, $P_{r,1}$ are the incident pressure and the reflected pressure on the surface between mediums 1 and 2, respectively. $P_{rad,1}$ is obtained by the Rayleigh integral [6].

$$P_{rad,1} = -\frac{j\omega\rho_0 V_{12} 2a}{2\pi} e^{-jk_x x} \int_{-\infty}^{\infty} \frac{\sin\alpha a}{\alpha a} \frac{e^{-j\alpha y + z\sqrt{\alpha^2-\gamma^2}}}{\sqrt{\alpha^2-\gamma^2}}, \tag{2.6}$$

where $V_{12}$ is the amplitude of the surface velocity between mediums 1 and 2, $2a$ is the width of a slit. $k_x$ denotes a wave number propagating along the strip

$$\gamma^2 = {k_0}^2 + {k_x}^2. \tag{2.7}$$

The pressure field in medium 2 comprises an in−coming wave and an out−going wave, —respectively. Assume that waves propagate constantly in the y−direction.

$$P_{i,2}(x,z) = \hat{P}_{\mathrm{i},2} e^{-jk_a(x\sin\theta_2 + z\cos\theta_2)} \text{ and} \tag{2.8}$$

$$P_{r,2}(x,z) = \hat{P}_{\mathrm{r},2} e^{-jk_a(x\sin\theta_2 - z\cos\theta_2)}, \tag{2.9}$$

where $k_\mathrm{a}$ represents the wave number of a slit with or without an acoustic seal. The transmitted field in medium 3 can be calculated by the Rayleigh integral as follows:

$$P_{rad,3} = -\frac{j\omega\rho_0 V_{12} 2a}{2\pi} e^{-jk_x x} \int_{-\infty}^{\infty} \frac{\sin\alpha a}{\alpha a} \frac{e^{-j\alpha y + z\sqrt{\alpha^2-\gamma^2}}}{\sqrt{\alpha^2-\gamma^2}}, \tag{2.10}$$

Eqs.(2.6) and (2.10)can be changed by the acoustic impedance formula

$$P_{rad,1} = -Z_{\mathrm{rad},1} V_{12} e^{-jk_x x}, \tag{2.11}$$

$$P_{rad,3} = Z_{\mathrm{rad},3} V_{23} e^{-jk_x x}\ , and \tag{2.12}$$

$$\begin{aligned} Z_{rad,1} = Z_{\mathrm{rad},3} = Z_0 \Big[ & H_0^2(2\gamma a) + \frac{\pi}{2}\big(H_1^2(2\gamma a) S_0(2\gamma a) \\ & - H_0^2(2\gamma a) S_1(2\gamma a) - \frac{1}{2k_0 a} H_1^2(2\gamma a) + \frac{2j}{\pi(2k_0 a)^2}\Big], \end{aligned} \tag{2.13}$$

where $H_{\mathrm{i}}^2, S_{\mathrm{j}}$ is 2nd order Hankel and Struve function.

The problem of obtaining the unknown pressure and surface velocity can be solved by boundary conditions between adjacent media. The conditions are force equilibrium and velocity continuity relations. First, force equilibrium is applied to the surface of adjoining media.

$$\left(2\hat{P}_1 - Z_{\mathrm{rad},1} V_{12} - \hat{P}_{i,2} - \hat{P}_{r,2}\right)\mathrm{S} = m_{12} \mathrm{S} \dot{V}_{12} \text{ and} \tag{2.14}$$

$$\left(\hat{P}_{i,2} e^{-jk_a d \cos\theta_2} - \hat{P}_{r,2} e^{jk_a d \cos\theta_2} - Z_{\mathrm{rad},3} V_{23}\right)\mathrm{S} = m_{23} \mathrm{S} \dot{V}_{23}, \tag{2.15}$$

where $\dot{V}_{12}, \dot{V}_{23}$ represents the surface acceleration between adjacent media and $d$ denotes the thickness of a slit. Next, velocity continuity relations apply in the same way.

$$\frac{\hat{P}_{i,2} - \hat{P}_{r,2}}{Z_{12}} = \frac{V_{12}}{\cos\theta_2} \text{ and} \tag{2.16}$$

$$\frac{\hat{P}_{i,2} e^{-jk_a d \cos\theta_2} - \hat{P}_{r,2} e^{jk_a d \cos\theta_2}}{Z_{23}} = \frac{V_{23}}{\cos\theta_2}. \tag{2.17}$$

Matrix form could be obtained by substituting Eqs.(2.14) ~ (2.17) into Eqs.(2.4) ~ (2.13)

$$\begin{bmatrix} 1 & 1 & a_{13} & 0 \\ 1 & -1 & a_{23} & 0 \\ a_{31} & a_{32} & 0 & a_{34} \\ a_{41} & a_{42} & 0 & a_{45} \end{bmatrix} \begin{Bmatrix} b_{11} \\ 0 \\ 0 \\ 0 \end{Bmatrix} = \begin{Bmatrix} \hat{P}_{i,2} \\ \hat{P}_{r,2} \\ V_{12} \\ V_{23} \end{Bmatrix}, \qquad (2.18)$$

where

$$a_{13} = Z_{rad,1} + j\omega m_{12}, \qquad a_{23} = -\frac{Z_{12}}{\cos\theta_2},$$
$$a_{31} = e^{-jk_a d\cos\theta_2}, \qquad a_{32} = e^{jk_a d\cos\theta_2},$$
$$a_{34} = -Z_{rad,3} - j\omega m_{23}, \qquad a_{41} = e^{-jk_a d\cos\theta_2},$$
$$a_{42} = e^{-jk_a d\cos\theta_2}, a_{45} = -\frac{Z_{23}}{\cos\theta_2}, and\ b_{11} = \frac{2\hat{P}_i \sin(k_0 a \sin\theta \sin\varphi)}{k_0 a \sin\theta \sin\varphi}.$$

The sound transmission coefficient in a slit is defined as follows:

$$\tau_{slit}(\theta_i,\varphi_i) = \frac{\Pi_t(\theta_i,\varphi_i)}{\Pi_i(\theta_i,\varphi_i)}, \qquad (2.19)$$

where $\Pi_i(\theta_i,\varphi_i), \Pi_t(\theta_i,\varphi_i)$ are incident power on the slit and transmitted power through the slit at angles $(\theta_i,\varphi_i)$, —respectively.

$$\tau_i(\theta_i, \varphi_i) = \frac{2a}{\left(\frac{|\hat{P}_i|^2}{2}\right)/Z_0} \cos\theta_2 \; and \tag{2.20}$$

$$\tau_t(\theta_i, \varphi_i) = \frac{1}{2} 2a \times Re(Z_{rad,3})|V_{34}|^2. \tag{2.21}$$

The diffuse field sound transmission coefficient could be represented numerically as follows:

$$\tau_d = \int_0^{2\pi} \int_0^{\theta_{lim}} \frac{\tau(\theta_i, \varphi_i) \sin\theta_i \cos\phi_i \, d\theta_i d\phi_i}{\pi \sin^2\theta_{lim}}, \tag{2.22}$$

where $\theta_{lim}$ is the limit angle that is different from the environment of an acoustical laboratory. The limit angle $\theta_{lim} = 70°$ was obtained to match the predicted STL with the measured one for the single partition in Figure 2.3. Eq.(2.22) can be changed by a simple relationship between the normal incident coefficient $\tau_o$ and the diffuse field transmission coefficient $\tau_d$ [1]. Thus, transmission loss is calculated as follows:

$$\tau_d = \frac{2(1 - \cos\theta_{lim})}{\sin^2\theta_{lim}} \tau_0 \; and \tag{2.23}$$

$$TL(\theta_i) = 10 \log_{10}\left(\frac{1}{\tau_d}\right). \tag{2.24}$$

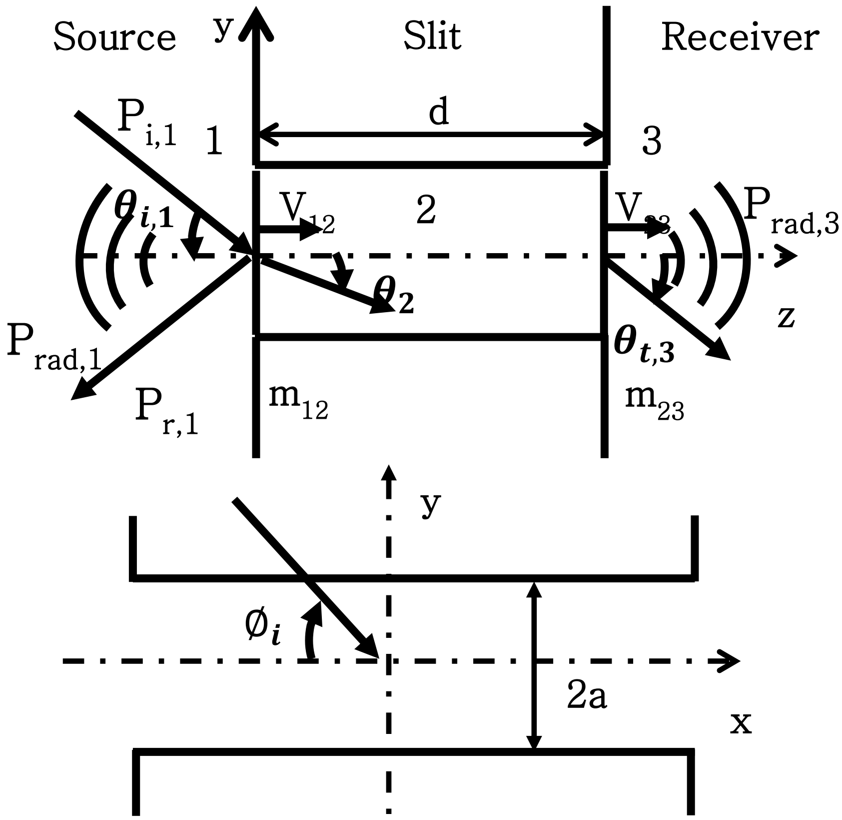


**Figure 2.2** —The transmission paths in cross section of a slit

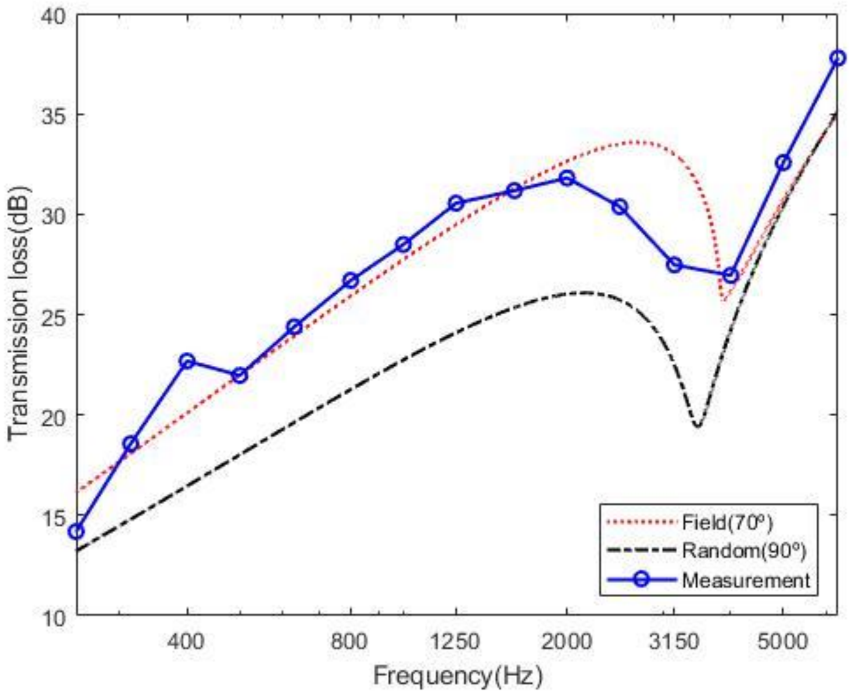


**Figure 2.3** —Mass law and measurement curve

# CHAPTER 3

# EXPERIMENT

## 3.1. Experimental arrangement

The sound intensity technique was utilized to measure the transmission loss of the wall with acoustic sealing. The measurements were implemented in the reverberant room and the semi−anechoic enclosure. The reverberant room was $241m^2$ and its cut−off frequency was $100\text{Hz}$. This location was outfitted with three diffuse microphones and two active loudspeakers that were separated from the wall to avoid a strong overlapping effect (see Figure 3.1). The semi−anechoic enclosure was employed with a sound intensity probe to gauge the sound intensity radiated from the slit in Figure 3.2.

The interconnected location of two rooms was tested with test samples of gypsum board with acoustic sealing. The samples size was $0.84 \times 0.84m^2$ and the slit width of samples was $5$ or $10\text{mm}$. The thickness of the slits was determined by the number of installed partitions, which were single or double partitions. The double partitioned cases were filled with mineral wool between the partitions, as shown in Figure 3.3. Table 3.1 represents the properties of samples.

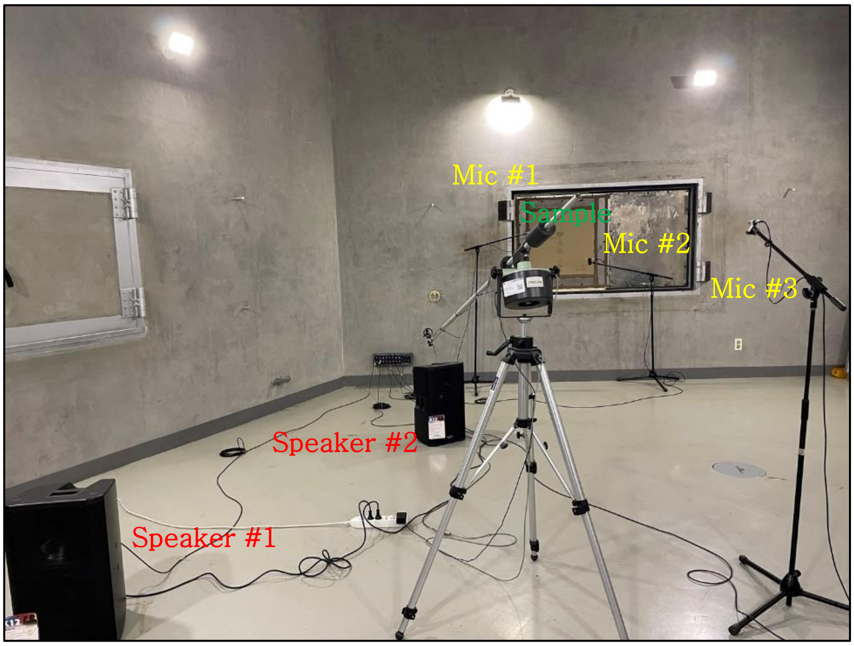


**Figure 3.1** —Reverberant room with installed equipment

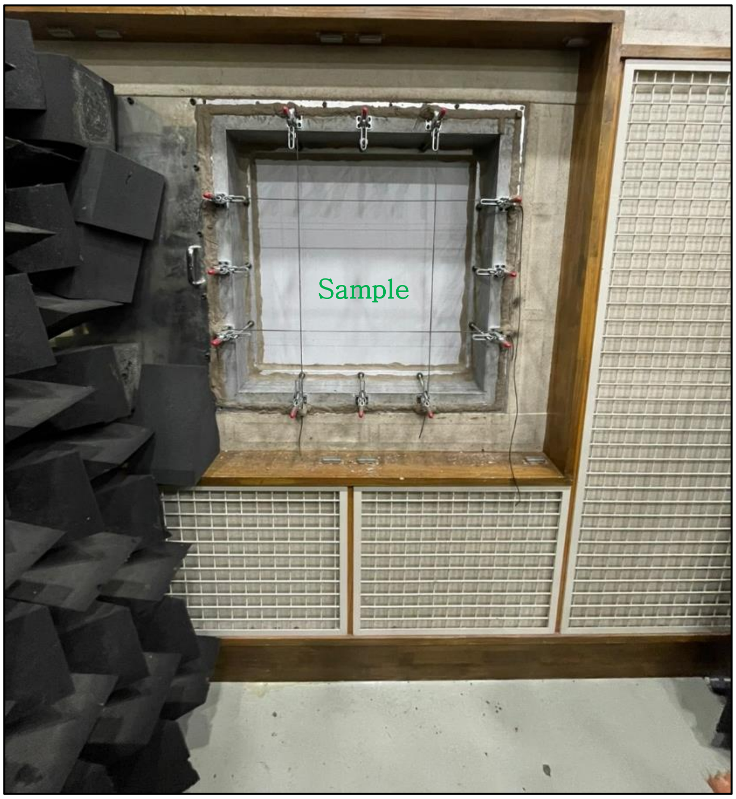


**Figure 3.2** —Semi-anechoic enclosure with installed sample

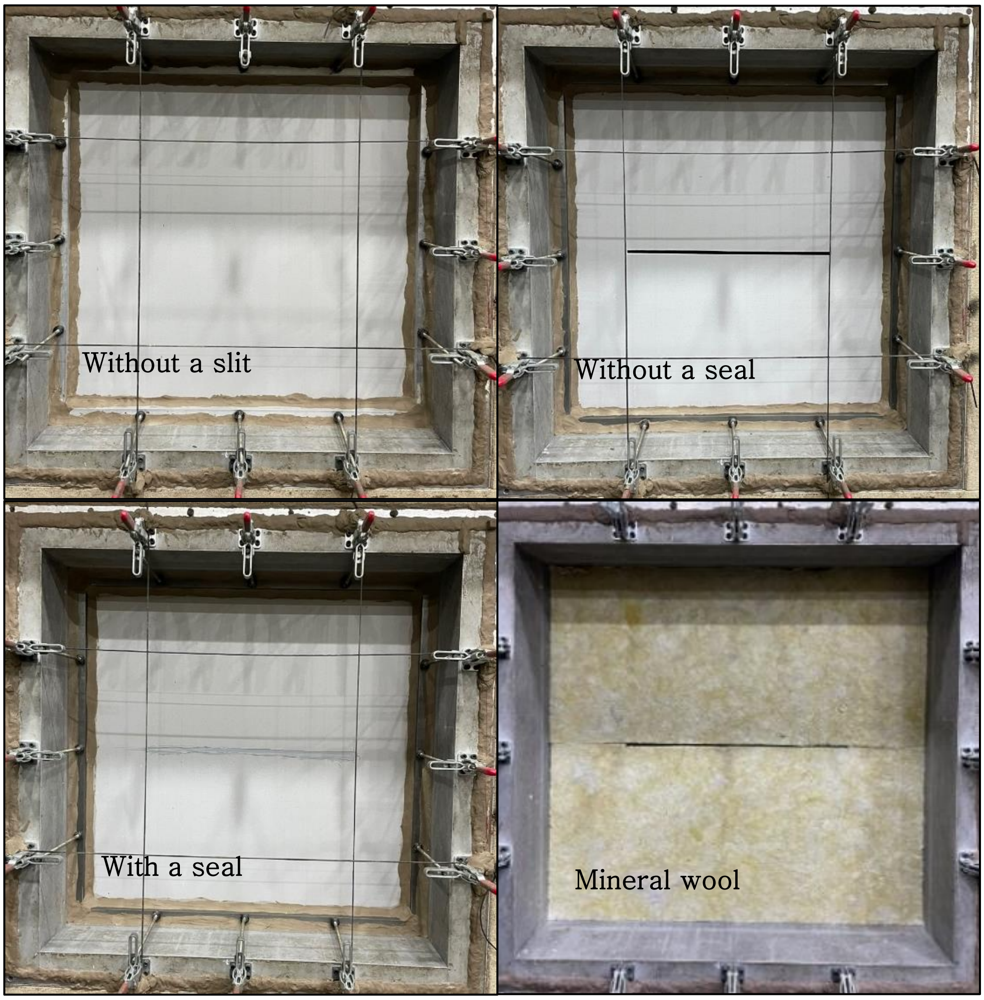


**Figure 3.3** —Test sample with/without acoustical seal and mineral wool

Table 3.1 —The material properties of test samples

| Materials | Properties | Values |
| --- | --- | --- |
| sealant | Surface density | 19.9kg/$m^2$ |
| | Young's modulus | $7.84 \times 10^5$Pa |
| | Thickness | 1p : 9.5mm |
| Gypsum board | Surface density | 5.20kg/$m^2$ |
| | Young's modulus | $2 \times 10^9$Pa |
| | Poisson ratio | 0.3 |
| | Thickness | 1p : 9.5mm |
| Mineral wool | Surface density | 1.50kg/$m^2$ |
| | Young's modulus | $1 \times 10^5$Pa |
| | Thickness | 25mm |
| | Flow resistivity | 16900 rayls/m |

## 3.2. Experimental results

Figures 3.4 and 3.5 show the transmission losses for single and double partitions with and without acoustic sealing, respectively.

The transmission loss of single partition with a slit tended to be unity as the frequency was higher, and to vanish the resonance effect in critical frequency which existed in single partition without a slit and with a seal.

$$f_{cr} = \frac{1}{2\pi} c^2 \left(\frac{m}{D}\right)^{1/2} \; and \tag{3.1}$$

$$D = \frac{Ed^3}{12(1-\nu^2)}, \tag{3.2}$$

where $D, \nu, \mathrm{E}$ denote the flexural rigidity, Possion's ratio, —and Young's modulus of the partition, —respectively. The wall with a slit had lower transmission loss than other cases, and the wider the width of the slit on the wall, the less transmission loss it had. On the other hand, the result of the transmission loss of the wall with a sealant was opposite to the prior results because the surface density of the sealant ($19.95 kg/m^2$) was larger than that of the gypsum board ($5.2 kg/m^2$).

Double partitions had the same consequences as single partitions in that the transmission loss of these tended to be higher as the frequency increased. All cases of double partitions have the same resonance frequencies, regardless of sealing. Mass−air−mass resonance frequencies $f_{mam}$ are identified near $200\,Hz$, and cavity resonance frequencies $f_{cavity}$ occur near $4{,}000\,Hz$ because of the same thickness of the cavity $d$. Eqs.(3.3) and (3.4) are defined as follows:

$$f_{mam} = \frac{1}{2\pi}\left[\frac{\rho_0 c^2}{d}\left(\frac{m_1 + m_2}{m_1 m_2}\right)\right]^{1/2} \sec\theta_1 \ and \qquad (3.3)$$

$$f_{cr} = \frac{\mathrm{cn}}{2d}\sec\theta_1 \ \ (n: integer), \qquad (3.4)$$

where $m_1, m_2$ denotes the surface density of gypsum board respectively, and $n$ is a positive integer.

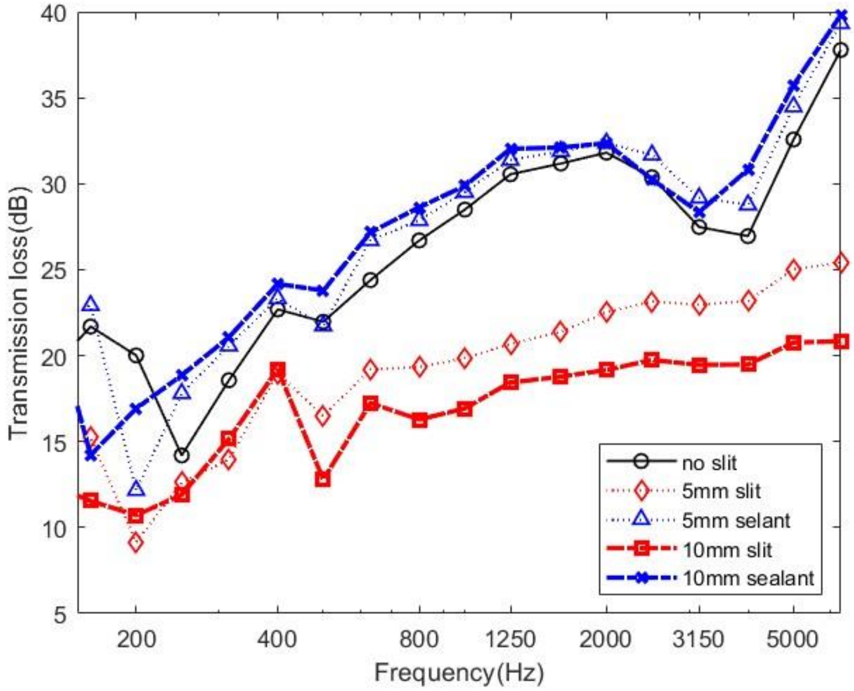


**Figure 3.4** —Measured transmission loss of the single partition

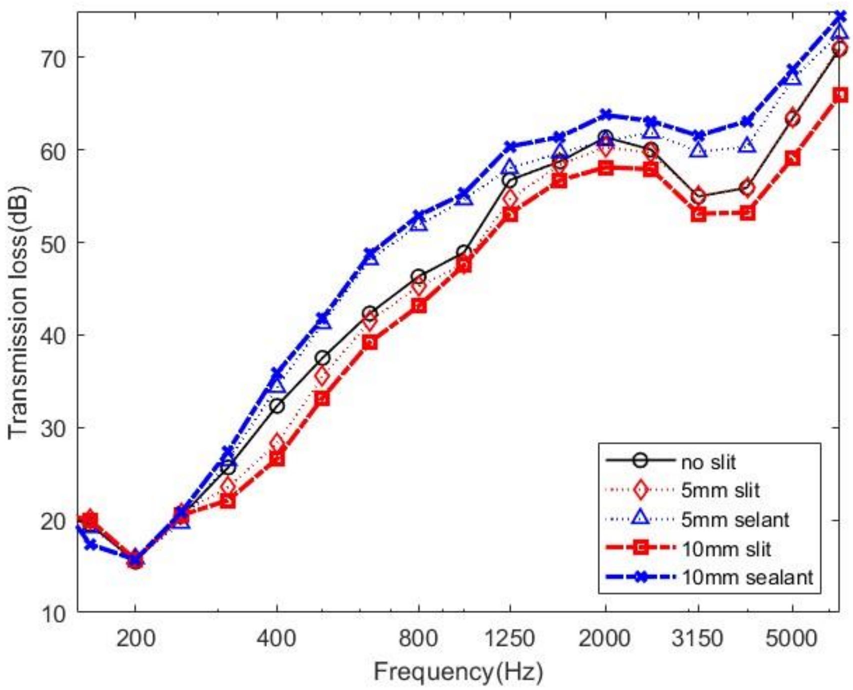


**Figure 3.5** —Measured transmission loss of double partitions

# CHAPTER 4

# RESULTS AND DISCUSSION

Figure 4.1 represents a comparison of transmission loss predicted by Gomperts and Kihlman [3] and Mechel [6] prediction models with observed transmission loss by adjusting the width of a slit for a single partition. Mechel' s model outperforms Gomperts' and Kihlman' s model The differences in transmission loss between the measured and the proposed models are within $2dB$ for the single partition with the slit.

The single partition with an acoustic sealant is represented in the same manner as Figure 4.2. The predicted transmission loss does not change compared to that in no a slit, but the measured one changes with a slight increase. Eq.(2.1) shows why the predicted model did not change when the transmission coefficients of the partition and the slit have no significant difference. The contribution of the slit is neglected because the area of the slit in Eq.(2.1) is very small compared to the area of the partition. As a result, the partition' s transmission coefficient can approximately represent the wall' s overall transmission coefficient as only it is significant. On the contrary, if the area of the slit increases significantly, the total transmission coefficient of the wall is affected, as shown in Figure 4.3.

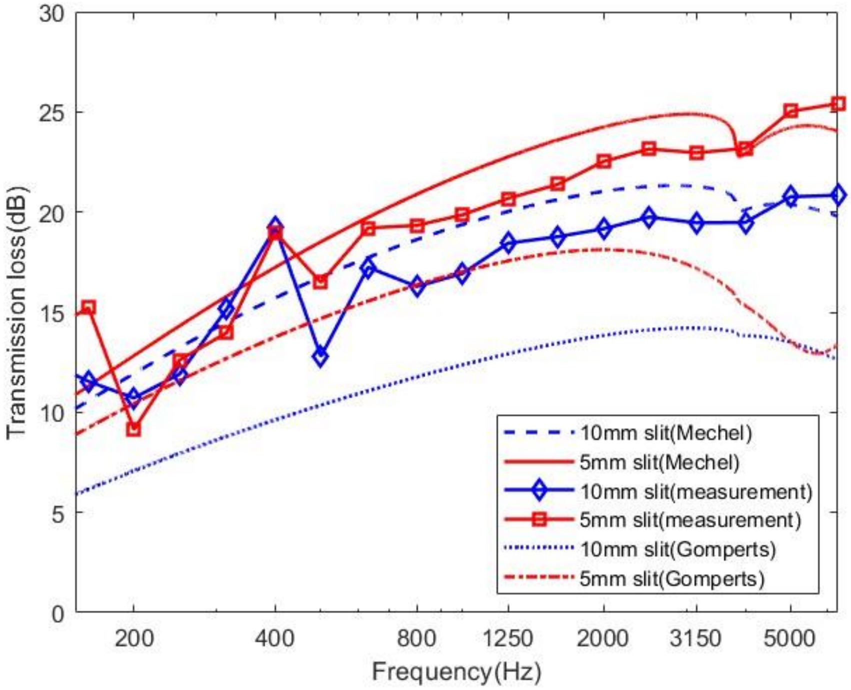


**Figure 4.1** —The comparison between measured transmission loss of the single partition with a slit and predicted models

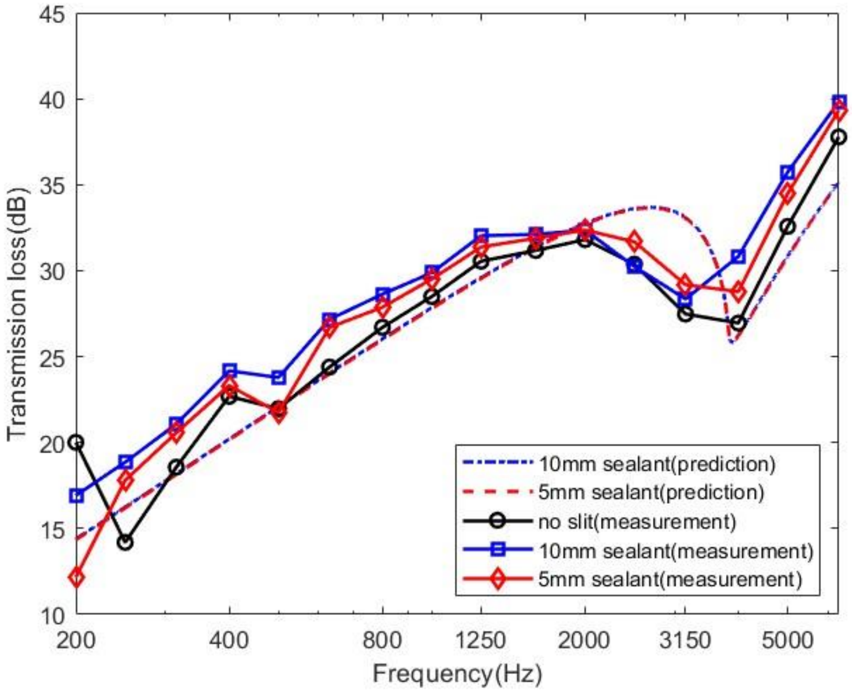


**Figure 4.2** —The comparison between measured transmission loss of the single partition with a sealant and predicted models (2a = 5, 10mm)

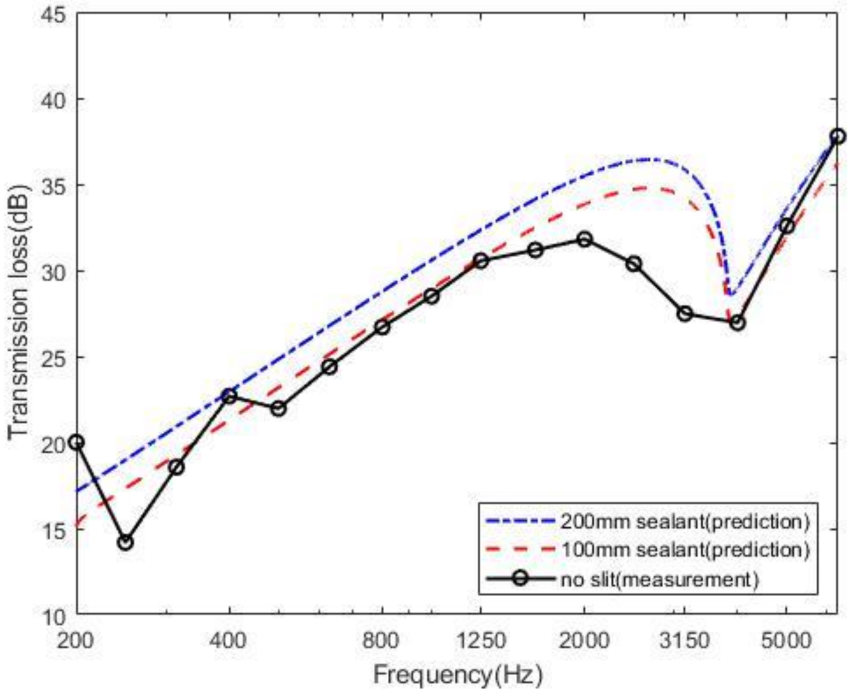


**Figure 4.3** —The comparison between measured transmission loss of the single partition with a sealant and predicted models (2a = 100, 200mm)

# CHAPTER 5

# CONCLUSION

This study presents a theoretical model that can predict the total transmission loss of a single partition with a slit. The theory uses a Mechel prediction model rather than Gomperts and Kiliman, which have been primarily employed in earlier studies. The proposed model has very good agreement with the measurement values, with a difference of less than $2dB$.

When the transmission coefficients of the partition and sealant do not differ significantly, the theory is limited. However, the slit with an acoustic sealant represents an equivalent sound reduction effect, which is a wall without a slit.

The predicted model will be validated using other various conditions, —such as the variety of partitions, sealing materials, and position of a slit. In addition, it will be necessary to develop a model for double partitions, which is not predicted in the above study. Finally, the contribution of the partition and the slit to sound reduction must be evaluated.

# REFERENCES

[1] Sgard F., Nelisse H., Atalla N., On the modeling of the diffuse field sound transmission loss of finite thickness apertures, J Acoust Soc Am 2007;122(1):302-13.

[2] Gomperts M. C., The “sound insulation” of circular and slit-shaped apertures, Acta Acust United 1964;14:1-16.

[3] Gomperts M. C., Kihlman T., The sound transmission loss of circular and slit-shaped apertures in walls, Acta Acust United 1967;37;286-297.

[4] Wilson G. P., Soroka W. W., Approximation to the diffraction of sound by a circular aperture in a rigid wall of finite thickness, J Acoust Soc Am 1965;37:286-97.

[5] Sauter Jr. A., Soroka W. W., Sound transmission through rectangular slots of finite depth between reverberant rooms, J Acoust Soc Am 1970;47:5-11.

[6] Mechel F. P., The acoustic sealing of holes and slits in walls, J Sound Vib 1986;111:297-336.

[7] Chen K. T., Study of acoustic transmission through apertures in wall, Appl Acoust 1995;46:131-51.

[8] Yang C., Zhang, X., Tao F., Lam D. C., A study of the sound transmission mechanisms of a finite thickness opening without or with an acoustic seal, Appl Acoust 2017;122:156-66.

[9] Park, H. H., Eom, H. J., Acoustic scattering from a rectangular aperture in a thick hard screen, J Acoust Soc Am 1997;101:595−8.

[10] Poblet−Puig J., Rodriguez−Ferran A., Modal−based prediction of sound transmission through slits and openings between rooms, J Sound Vib 1993;161:119−35.

[11] Oldham D. J., Zhao X., Measurement of the sound transmission loss of circular and slit−shaped apertures in rigid walls of finite thickness by intensimetry, J Sound Vib 1993;161:119−35.

[12] Hongisto V., Keranen J., Lindgren M., Sound insulation of doors−Part 2:comparision between measurement results and predictions, J Sound Vib 2000;230:133−48.

[13] Uris A., Bravo J. M., Llinare J., Estelles H., The influence of slits on sound transmission through a lightweight partition, Appl Acoust 2004;65:421−30.

[14] Kim M. J., An J. H., Effect of slit−shaped apertures on sound insulation performance of building elements, Noise Control Eng J 2009;57:515−23.

[15] Fahy F., Gardonio P., Sound and structural vibration: radiation, transmission and response, 2$^{nd}$ ed, Academic Press; 2007.

# 국 문 초 록


실내에 공간을 구분하고 소음을 차단하는 목적으로 쉽게 설치가능한 것이 경량 벽체이다. 경량 벽체는 비내력벽으로 기존 구조물과 별도로 구조물을 설치되기 때문에 접합부에 틈새가 생기기 마련이다. 이 틈새는 천정과 바닥 또는 창문, 문 등이 해당되며, 이 틈새는 방음과 방화성능에 방해가 되기 때문에 실란트 시공을 통해 틈새를 메우게 된다. 실란트 중 방음용 실란트는 벽 틈새를 채워 인접한 공간 상에서 발생하는 소음을 차단하는 역할을 한다.

본 연구는 경량 벽체 상 틈새 소음에 대해서 실란트 유무에 따라 음향 투과를 이론적 분석을 목적으로 실시하였고, Sound intensity technique을 이용한 투과손실 측정을 통해 이론의 타당성을 검증하였다. 이전 연구부터 이론적 모델로 주로 사용되었던 Gomperts와 Kiliman의 예측 모델이 아닌 Mechel의 예측 모델을 활용하였고, 실험결과와 비교하여 어느 모델이 더욱 타당한지도 확인하였다. 중 · 고주파수 대역에서 Mechel의 예측모델이 측정결과에 근접하였고, 이 모델을 통해 측정결과 대비 $2dB$ 이내의 근접한 결과를 예측하였다. 반면, 이론적 모델에서는 벽과 실란트 투과계수가 현저히 차이가 나지 않는다면 투과손실이 예측이 제한되는 점이 식별되었지만 실란트로 틈새를 채웠을 때 틈새가 없는 벽과 유사한 방음성능을 발휘한다는 것을 알 수 있었다.



주요어 : 실내소음, 측면 투과, 틈새, 방음 씰

학　번 : 2021-27018